JOURNAL OF OPTOELECTRONICS AND ADVANCED MATERIALS Vol. 10, No. 8, August 2008, p.2061 - 2067

Plasma and laser processing of YZT materials for sensor applications

B. MITU[a*], S. SOMACESCU[b], M. FILIPESCU[a], P. OSICEANU[b], V. PÂRVULESCU[b], M. DINESCU[a], G. DINESCU[a],
[a]*National Institute for Lasers, Plasma and Radiation Physics, PO Box MG-16, 077125 Magurele Bucharest, Romania*
[b]*Institute of Physical Chemistry, Spl. Independentei 202, Bucharest, Romania*

Ternary oxides of zirconium, yttrium and titanium were obtained by hydrothermal method in powder form and respectively as thin films by pulsed laser deposition, under different concentrations of TiO_2. The materials were investigated regarding their morphology, topography, chemical and structural characteristics. Electrical measurements were performed in order to asses their use in toxic gas sensors. A parametric range of experimental conditions corresponding to a maximum sensitivity to NO_x toxic gas has been established for the thin films deposited by pulsed laser deposition.

(Received March 1, 2008; accepted June 30, 2008)

Keywords: Ternary oxides ZrO_2 - Y_2O_3 - TiO_2, Hydrothermal synthesis, Pulsed laser deposition, RF assisted pulsed laser deposition, Gas sensors

1. Introduction

The complex nanostructured oxides are used in a wide range of applications in optic, catalytic [1], biomedical [2] fields or in sensing applications [3]. The properties of yttria stabilized zirconia (YSZ), like high dielectric constant [4], or low thermal expansion coefficient [5] make the material suitable for gate dielectrics, solid electrolytes for sensors or fuel cells or for use as buffer layer of superconducting coatings [5]. The addition of other metals or oxides in the structure of yttria stabilized zirconia can enhance some properties, like conductivity or toughness [7]. Particularly, the mixed yttria stabilized zirconia and titania combine the high ionic conductivity of the oxygen with the chemical and mechanical energy of the oxide, leading to long-term stability of anode materials in SOFC [8].

In this contribution, a complex investigation of ZrO_2 - $8\%Y_2O_3$- $x\%TiO_2$ (x in the range 10-30) material obtained in powder form by hydrothermal method and as thin film by pulsed laser deposition method has been performed. The chemical, structural, and morphological properties are reported. The electrical response of the deposits to NO_x toxic gas was evaluated.

2. Experimental

The ternary oxides, $ZrO_2 - 8\%Y_2O_3 - x\%TiO_2$, with x = 8, 10, 15, 30 % TiO_2, were synthesized by hydrothermal treatment. The reagents used for synthesis were cetyltrimethylammonium bromide (CTABr, Aldrich) as the surfactant, Zirconium oxychloride ($ZrOCl_2$, Riedel de Haën) yttrium nitrate hexahydrate ($Y(NO_3)_3 6H_2O$, Merck), titanium (IV) isopropoxide (Fluka) as inorganic precursors, urea 99.8% (Alpha Aesar) as hydrolyzing agent and tetrametyilammonium hydroxide (TMAOH solutions 25 wt. % in water, Aldrich) as precipitate agent. The molar ratio of oxide/surfactant/urea was 1: 0,36: 7. An aqueous solution of inorganic precursors was introduced by dropwise to a mixture of 2.8g CTMABr and 60 ml H_2O, after 2h stirring. Subsequently, urea was added and reaction proceeded at 80 ^oC for 4h, under stiring and refluxing conditions. The pH was adjusted at 9 using a tetrametyilammonium hydroxide (TMAOH) and the precipitate has been loaded into Teflon link steel autoclave and heated at 373 K for 3 days. All the products were filtered, washed, dried at 373 K and calcinated in N_2 flow and then air at 823 K.

The so-obtained ZrO_2 - $8\%Y_2O_3$- $x\%TiO_2$ powders have been further processed by pressing in pellets on a pressure of 25 $x10^5$ Pa in order to obtain targets for the laser ablation experiments. A soft thermal treatment on a temperature of 873 – 973 K has been applied for insuring a compact and dense structure of the targets.

The pulsed laser deposition experiments, with or without RF plasma assistance, have been performed by irradiating the targets with the fourth harmonic of a Nd: YAG laser (wavelengths 266 nm, pulse length 5 ns, repetition rate 10 Hz, number of pulses 20000). The laser beam was focused at 45^o incidence on the targets, which were mounted on a rotation-translation stage in order to prevent the fast drilling. The laser fluence was kept constant at 3 J\cm^2. Si(100) substrates have been placed at 4 cm in front of the target and maintained at room temperature during deposition. A base pressure of 10^{-2} Pa was insured prior deposition by an assembly consisting of a rotative and a turbomolecular pump, while the pressure during deposition was established at 5 Pa, under constant

oxygen flow and constant pumping speed. For improving the species reactivity at the substrate level, the PLD set-up has been improved by assisting the deposition process with an oxygen radiofrequency plasma beam [9]. The RF discharge, generated at 100 W in flowing oxygen between two parallel electrodes, is expanding into the ablation chamber as a plasma beam through an aperture performed in the bottom electrode [10]. The thin film growth is a complex process in which the species originated from the laser plasma plume (Zr, Ti, and Y atoms, ions, radicals, etc.) and the oxygen species generated by the RF discharge contribute to form the compound consisting of the three oxides (yttria, titania and zirconia.)

The powders obtained by hydrothermal treatment were characterized by Scanning Electron Microscopy (SEM) with a Philips XL-20 microscope. The surface topography of the thin films obtained by (RF-) PLD has been examined by Atomic Force Microscopy (AFM) method. A Quesant Scan Atomic instrument working in air, in the wavemode, was scanning the surfaces over 20x20 μm^2.

The XRD pattern was recorded on a DRON DART UM-2 diffractometer equipped with a Cu Kα radiation and a graphite monochromator in the diffracted beam. A step scanning technique was applied with a step width of 0.05^0 and an acquisition time on each step of 2 s, ranging from $2\theta=10\text{-}70^o$.

Surface analysis performed by X-Ray Photoelectron Spectroscopy (XPS) was carried out on VG Scientific ESCA-3 equipment, with a base pressure in the analysis chamber of 10^{-9} mbar. The nonmonochromatized AlK radiation (1486.6eV) was used as X-ray source. The overall energy resolution is estimated at 1.2eV by the full width at half maximum (FWHM) of the $Au4f_{7/2}$ line. In order to take into account the charging effect on the measured Binding Energies (BEs), the spectra were calibrated using the C1s line (BE = 284.6eV) of the adsorbed hydrocarbon on the sample surface. All the samples were characterized in the "as received" stage, without any Ar ion cleaning procedure. For the powders analysis, they were pressed on an In foil.

In order to asses the material as useful in detection of toxic gases, electrical measurements of the samples have been performed by dc two-point probe using a Fluke 789 Processmeter. The resistance measurements were carried out at room temperature, in a glass cell containing NO_x at a concentration level $5x10^{-3}$ $mol.l^{-1}$. By monitoring in time the modification of the samples resistance during NO_x exposure, the sensitivity to the toxic gas has been evaluated.

3. Results and Discussion

3.1. Samples morphology and topography

Scanning electron microscopy (SEM) images of the ternary oxides obtained by hydrothermal route show a morphology characteristic to mesoporous materials. In Fig. 1 is presented a picture corresponding to the powders synthesised with 10% amount of TiO_2: the material consists of globular particles of hundreds of nanometers .

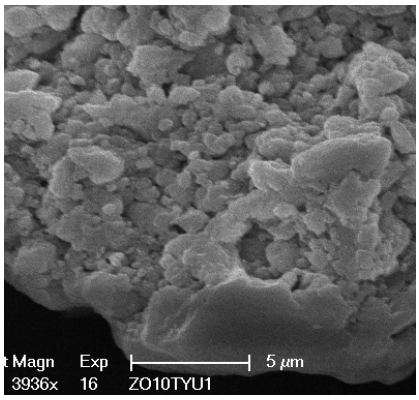

Fig.1. Typical SEM picture of the powders synthesized by hydrothermal route

The thin films obtained by (RF)-PLD starting from these powders present a surface topography dependent on the deposition conditions. In Figure 2 are presented images from samples deposited by classical PLD (a) and RF-assisted PLD (b) from ZrO_2 - 8%Y_2O_3- 15%TiO_2 target. The surface topography of the sample deposited by classical PLD (Figure 2a) is typical for all the samples, regardless the TiO_2 percentage in the target (in the range 10 – 30%). They show a granular structure, corresponding to a large superficial area for adsorbing the NO_x molecules, and a roughness in the range of 3 - 5 nm. The RF addition (Figure 2b) induces a smoother surface, with the RMS value lower than that of the classical PLD. A few particulates of approximately 100 nm are present on the surface. In Figure 3 are presented the surfaces of the samples obtained by RF – PLD starting from 10% and respectively 30 % of titania in the target. The surface of the sample with the lowest amount of titania is the smoothest one, with RMS~ 1.5 nm, while by increasing the titania content in the target, the surface become more rough, reaching RMS ~ 10.5 nm for 30% TiO_2. The increase of the roughness seems to be determined by the increase number of the particulates on the surface, which may correlate to the formation of a different phase of the material when the TiO_2 concentration is increasing.

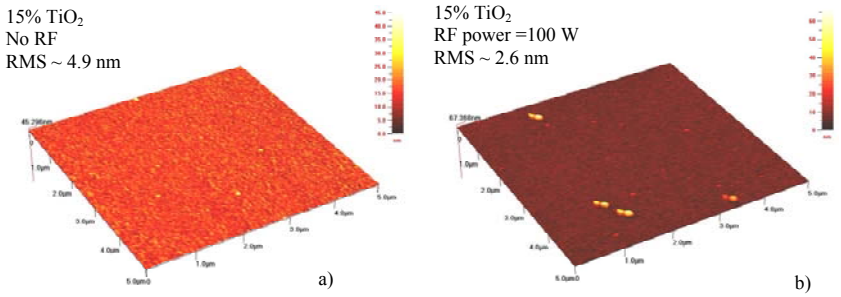

Fig. 2. AFM images of the samples deposited starting from powders with 15% TiO_2; a) classical PLD; b) RF assisted PLD (100 W).

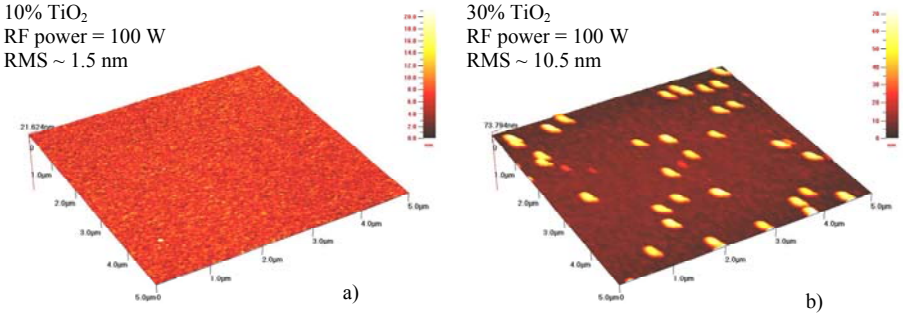

Fig. 3. AFM images of RF – PLD samples (100 W) deposited from powders with a) 10% TiO_2; b) 30% TiO_2

3.2. Structural properties

An extensive investigation of the structural properties of the ZrO_2 - $8\%Y_2O_3$- $x\%TiO_2$ powders, the corresponding targets and the deposited thin films has been realized by XRD technique. The crystalline phase identification was done by using JCPDS database files system. Profile-fitting calculations were performed using Voigt functions. The crystallite sizes were calculated from the corrected FWHM (full width at half maximum) applying the Debye-Scherrer formula. The XRD patterns for the as-prepared powders and the obtained targets are displayed in Figure 5. The absence of peaks in the 2θ = 40-50^o region guides us to consider as predominant phase a cubic one. However, the asymmetry of the 200, and 311 peaks in the powders (indicated by arrows in Fig. 5a), which is more prominent for the sample with 30% TiO_2 amount, suggests the presence of a tetragonal phase also, difficult to be extracted due to the overlapped of the peaks. The XRD spectra of the targets (Fig. 5b) exhibit, besides the predominant cubic ZrO2-phase, a lower amount of tetragonal phase which could be more likely assigned to a monoclinic ZrO_2-like phase. In the corresponding diffractograms, the additional peaks have been denoted with stars.

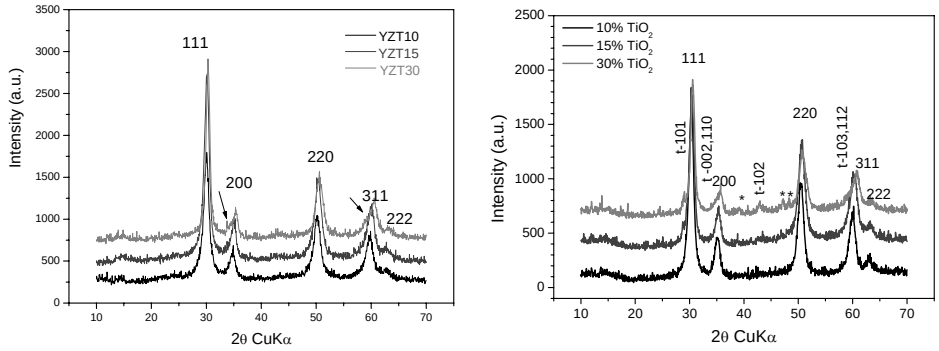

Fig. 5. X-ray diffractograms of the powders (left) and of the targets (right)

The values of the unit cell parameter **a** and of the average size of the crystallites **D** are presented in Table 1. The decrease of the unit cell parameters as the TiO_2 amount increases indicates the substitution of Zr^{4+} with Ti^{4+} in the crystal, since the Shannon ionic radius for Ti^{4+}, of 0.605 Å, is lower than that of Zr^{4+}, of 0.72 Å [11]. A similar trend is observed also for the targets, but slightly lower values are obtained for all the samples probably due to the departure of some ZrO_2 in the observed tetragonal phase. Moreover, the Ti incorporation seems to lead to an increase of the mean crystallites sizes **D**, which is even more pronounced for the targets, probably due to the annealing procedure. The thermal treatment of the corresponding target led to a well crystallized material, but with a significantly larger unit cell parameter. This suggests further rearrangements in the network during annealing procedure, as if the cerium ions occupied the framework positions.

*Table 1. The values of the calculated unit cell parameter **a** (Å) and the average crystallite size **D** (nm)*

	Sample	TiO_2 (weight %)	a (Å)	D (nm)
powders	YZT10	10	5.150	6.7
	YZT15	15	5.132	7.4
	YZT30	30	5.099	9.8
targets	YZT10	10	5.112	7.9
	YZT15	15	5.093.	8.6
	YZT30	30	5.062	9.7

It is worth noticing that the thin films obtained by pulsed laser deposition with or without RF assistance did not show any peak in the diffractograms; they are either amorphous, or too thin for giving signal to the X-ray analysis.

3.3. Chemical composition of the material

The chemical shifts in the BE's states of C1s, O1s (singlet), Ti2p, Y3d and Zr3d doublets states provide information about the oxidation states. Quantitative information regarding the elemental relative concentrations in the samples has been obtained by processing the XPS spectra.

The surface composition has been determined as relative element concentrations (atom %), from the relative area intensities of different high-resolution peaks, after normalization by their sensitivity factors and after corrections for transmission function, escape depth and detector efficiency. It must be outlined that under XPS conditions the detected volume of our samples (either in powder or thin film form) is ranging in the first 20-25 monolayers meaning the only 4-5 nanometers below the surface which, obviously, can be different from the bulk composition.

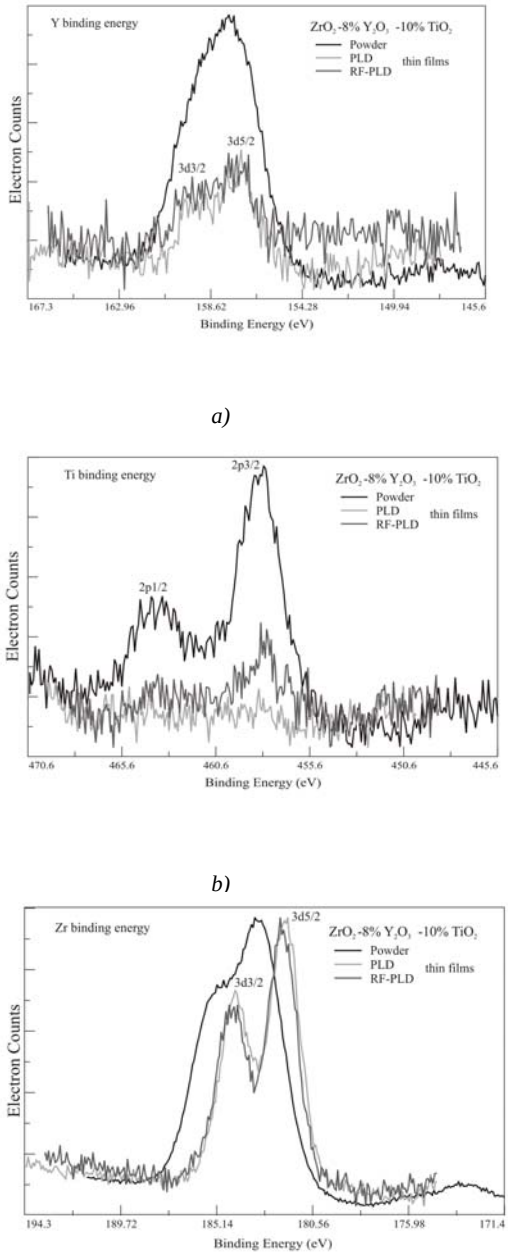

Fig. 6. XPS spectra of the ZrO_2 - 8%Y_2O_3- 10%TiO_2 material as powder and thin films deposited by (RF)-PLD corresponding to the binding energies of a) Y; b) Ti; c)Zr.

In figure 6 are presented the XPS spectra of the samples (as powder and thin solid films deposited by (RF)-PLD) with hypothetical composition ZrO_2 - 8%Y_2O_3- 10%TiO_2, in the binding energy regions corresponding to Ti, Y and Zr. By investigating the

chemical environment of these elements, it could be identified the full oxidation state as TiO_2 and Y_2O_3 (see Fig. 6 a) and b)). As can be seen from Fig. 6c), a significant difference was signaled for the Zr behavior from the powder to the thin film. Thus, the Zr3d photoelectron peaks (3d3/2 = 183.03eV and 3d1/2= 185.45eV) in the ZrO_2 - 8%Y_2O_3- 10%TiO_2 powder was shifted with about 1eV towards higher binding energies in respect to the position corresponding to the ZrO_2 environment. This finding suggests a residual chemical bonding with chlorine atoms (electronegative element in respect to oxygen) from the oxychloride precursor. In the samples deposited by PLD and RF PLD starting from this powder, the supposed Zr-Cl chemical bond is broken and Zr exhibits its 4+ oxidation state, as ZrO_2. This effect is explained by the ablation process of the target, which leads to the break of the bonds and the decomposition of the target down to the atoms, the chlorine being exhausted by the pumping system.

In all the analyzed samples, the oxygen is found in excess as a result of the chemical bonding with carbon as OH-C-O, C=O or even as a result of some carbonyl (CO_3) groups partially coordinated by Ti and Zr. It must be emphasized that all the mentioned oxides are buried under the top surface which is covered by a carbon layer with a depth of 3-4 nm and which is not bound with any metal ion (no trace of carbides was found).

The following conclusions arise: in the "as received samples", carbon (ranging from 40 to 60%) and oxygen (25-45%) are the main surface components. The large amount of carbon found on the top of the surface is obviously related to the presence of organic contaminants due to incomplete metallorganic precursor decomposition as well as segregation of the carbon from the bulk to the surface during thermal treatment. After Carbon removal from the total stoichiometry of the samples, the relative concentrations of oxygen, titanium, yttrium and zirconium have been determined. The results for the material with the hypothetic ZrO_2 - 8%Y_2O_3- 10%TiO_2 stoichiometry are presented in Table 2. One must notice that during hydrothermal synthesis the oxygen is in excess, while the Ti and Zr are deficient in respect to the theoretical values. The use of classical PLD lead to a further decrease of the Ti concentration, below the detection limit, while the RF assisted PLD method conduct to samples with oxygen in excess, but with an overal composition of metals more similar to the hypothetical one (Zr/Y/Ti = 74.21/16.84/8.95 as compared to 75.73/14.91/9.36 in the ideal composition).

Table 2. Atomic concentration of the ZrO_2 - 8%Y_2O_3- 10%TiO_2 as determined by XPS for different synthesis conditions

Element / Sample	O(atom%)	Ti(atom%)	Y(atom%)	Zr(atom%)
Powder form	71.2	1.8	4.8	22.2
Thin film - PLD	58.2	-	7.7	34.1
Thin film RF - PLD	81	1.7	3.2	14.1
theoretical values	65.8	3.2	5.1	25.9

3.4. Response to toxic gas (NO)

The toxic gas selected for detection tests was NO_x. The sensitivity was defined as the ratio $\Delta R/R_{air}$, $\Delta R = R_{air} - R_{NOx}$ where R_{air} and R_{NOx} are the electrical resistance of the sample in dried air and after NO_x gas introduction, respectively. The response has been analysed both for the powders and for the thin films. In Figure 7 are presented the results for the ZrO_2 - 8%Y_2O_3- x%TiO_2 powders and thin films deposited by classical PLD. For the powders, the fastest response is obtained for the material with the highest percentage of TiO_2 (4 min after NO_x injection), while the thin films present an almost instantaneous response (in a few seconds) for lower values of TiO_2 content. In the case of thin films, another important parameter is governing the sensitivity to toxic gases, namely the surface roughness. Indeed, the sample with 15% TiO_2, which has the highest roughness value (~ 5 nm) has the best sensitivity.

One way to modify the surface roughness while keeping the same composition of the starting target is the RF addition during the deposition process. For low TiO_2 content, the RF assistance lead to a smoother surface, and correspondingly the response is getting worse (Figure 8a). Instead, if the TiO_2 concentration increases, which is equivalent to the apparition of new crystalline phases in the starting powder and target, some particulates appear on the surface and the film RMS starts to increase (Figure 8b). Still, in absolute values, the lower TiO_2 content seems favorable.

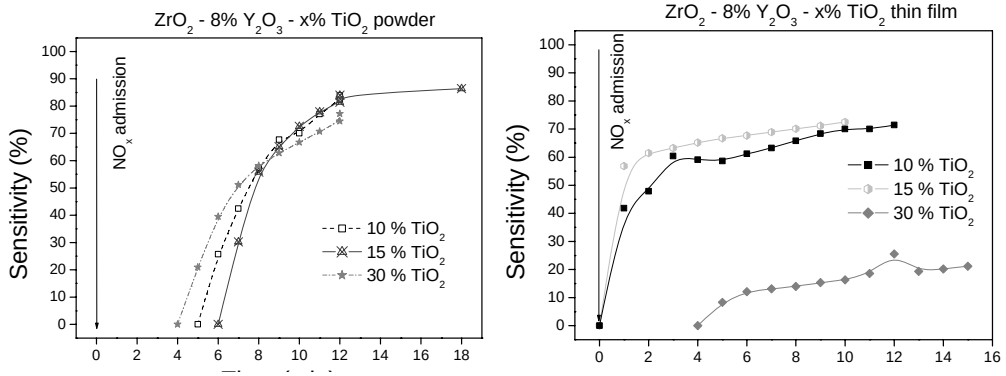

Fig. 7. Sensistivity of ZrO_2 - 8%Y_2O_3- x%TiO_2 powders and thin films obtained by classical PLD

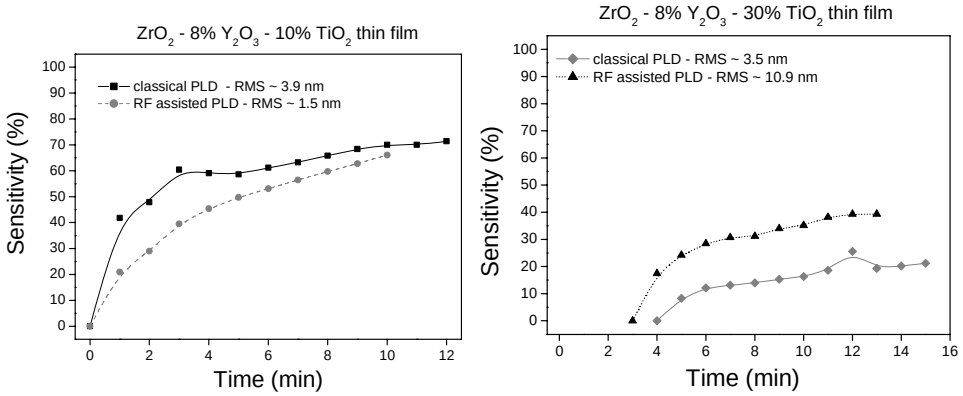

Fig. 8. Comparison of the sensitivities of ZrO_2 - 8%Y_2O_3- x%TiO_2 as function of TiO2 percentage and the addition of RF

4. Conclusions

Yttria titania stabilized zirconia material has been obtained in powder form by hydrothermal route and as thin films by pulsed laser deposition with or without additional RF plasma beam assistance. The chemical synthesis led to a material crystallized predominantly in cubic phase with crystallites dimension increasing with the TiO_2 content in the sample, while the targets prepared to be used in PLD showed the presence of a tetragonal phase, too. The YZT powders have a typical morphology for a mesoporous structure, while the thin films show a topography which is dependent on titania concentration and the RF addition. The XPS measurements on the ZrO_2 - 8%Y_2O_3- x%TiO_2 thin films have shown the presence of the oxides in their fully oxidized states, even if in the starting target some shift of the binding energy has been noticed for the Zr spectrum. Instantaneous responses to the NO_x toxic gas have been obtained for the pulsed laser deposited films in selected conditions. Two different mechanisms seems to be involved in the NO_x adsorption: one is related to the material composition, namely to the TiO_2 percentage, while the other one is related to the surface roughness, which can be varied by working in classical PLD or RF assisted PLD configurations.

Acknowledgement

One of the authors (B.M.) gratefully acknowledges the NATO support under the Reintegration grant EAP.RIG.981644.

References

[1] V. Pârvulescu, V. I. Pârvulescu, P. Grange, Catal. Today, **57** 193 (2000).
[2] H. Szymanowsky, A. Sobczyk, M. Gazicki-Lipman, W. Jakubowski, L. Klimek, Surf. Coat. Tech. **200** 1036-1040 (2005).
[3] O.K. Tan, W. Cao, Y. Hu, W. Zhu, Sol. St. Ionics **172,** 309-316 (2004).
[4] J. Zhu, Z.G. Liu, Mat. Lett. **57** (26), 4297 (5) (2003).
[5] H. Hayashi, T. Saitou, N. Maruyama, H. Inaba, K. Kawamura, M. Mori, Solid State Ionics, **176**, 5-6, 613-619 (2005).
[6] Y.M. Lai, P.A. Lin, C.C. Chi, J. Phys. D: Appl. Phys. **40** 3670-3673(2007).
[7] A.A. Voevodin, J.J. Hu, J.G. Jones, T.A. Fitz, J.S. Zabinski, Thin Solid Films, **401**, 1-2, 187-195 (2001).
[8] J. Will, A. Mitterdorfer, C. Kleinlogel, D. Perednis, L.J. Gauckler, Solid State Ionics, , **131** 79–96 (2000).
[9] M. Filipescu, N. Scarisoreanu, D.G. Matei, G. Dinescu, A. Ferrari, M. Balucani, O. Toma, C. Ghica, L.C. Nistor and M. Dinescu, Mat. Sci. Semic. Proc., **7**, 209-214 (2004).
[10] G. Dinescu, B. Mitu, E. Aldea, M. Dinescu, Vacuum, **56**,1 83-86 (2000).
[11] R. D. Shannon, Acta Crystallogr. **A32** 751 (1976).

*Corresponding author: mitub@infim.ro